Fatigue Behaviour of DLC Coated Die Material

K. Maruchi, Y. Uematsu, K. Tokaji
Gifu University, Gifu, Japan

1. Introduction

Tool alloys are wildly used as forming die materials because of their good hardenability by quenching and abrasive wear properties. Usually, die lubricant is used during forming process in order to avoid seizing and/or galling. Recently, however, it is known that the disposition of die lubricant as industrial waste is costly and detrimental to the environment, and dry forming process without lubricant is strongly required. Diamond-like carbon (DLC) film exhibits excellent properties such as high hardness, high coating adhesion, low defect density and chemical inertness. Furthermore, DLC film has very low coefficient of friction and high tribological properties [1], and is a strong candidate for the surface modification method of die materials for dry forming process. Recently, it is known that forming of complicated shape components induces the transition of localized stress field at the stress concentration part of dies from compression to tension during forming process. Therefore, it is very important to understand fracture mechanisms of DLC coated die materials under cyclic tension-compression loading patterns.

In this study, DLC film was deposited on two die materials, which were denoted as SKD11 and SKD61 by Japanese Industrial Standard (JIS), with two different thicknesses of 1μm and 15μm. Rotary bending fatigue tests have been performed and the effect of DLC coating on fatigue behaviour was discussed.

2. Experimental procedures

2.1 Materials

The materials used are tool alloys SKD11 and SKD61 whose chemical compositions (wt.%) are listed in Table 1. Using as-received round bar samples with the diameter of 13mm, both alloys were solution treated at 1030ºC for 15 minutes followed by quenching in air. Then SKD11 was tempered at two different temperatures of 500ºC and 600ºC for 60 minutes and air cooled, while SKD61 was only at 600ºC. SKD11 tempered at low and high temperatures are denoted as SKD11-LT and SKD11-HT, respectively. The microstructures of SKD11 and SKD61 are shown in Figs.1 and 2, respectively. In SKD11, large chromium carbides are recognized within the tempered martensitic microstructure, where the size of carbides is up to 60μm. The effect of tempering temperature on the

Table 1 Chemical composition of materials.

	C	Si	Mn	P	S	Cu	Ni	Cr	Mo	V
SKD11	1.45	0.3	0.36	0.027	0.001	—	—	11.51	0.82	0.22
SKD61	0.37	0.91	0.44	0.021	0.002	0.06	0.13	5.3	1.21	0.8

microstructure is not recognized in SKD11. On the other hand, the microstructure of SKD61 is the uniform tempered martensite without large carbides.

2.2 Procedures

The smooth round bar specimens with 5mm diameter and 5.04mm gauge length were cut from the heat-treated bars, and mechanically polished by emery paper and then buff-finished. DLC film was deposited on the gauge part of the specimens by means of a plasma enhanced chemical vapour deposition (PECVD) method with two different thicknesses of 1μm and 15μm. Rotary bending fatigue tests were performed at a cyclic frequency of 57 Hz in laboratory air at ambient temperature using bare and DLC coated specimens. Hardness was measured by means of a micro-Vickers hardness tester at a load of 9.8N at twenty points on the cross section. Residual stresses on specimen surface were evaluated by an X-ray diffractometer.

3. Experimental Results

3.1 Hardness and residual stress

The average of Vickers hardness at 20 points on the cross section is 650 and 464 for SKD11-LT and HT, respectively, and 530 for SKD61. The residual stress on the specimen surface is -843±118MPa and -210±76MPa for SKD11-LT and HT, respectively, and -213±78MPa for SKD61. The compressive residual stress could be introduced by both heat treatment and machining process. But, the machining of the specimen was performed after heat treatment so that the residual stress could be attributed mainly to the machining process.

3.2 SKD11

3.2.1 Fatigue strength

Fig.3 indicates *S-N* diagram of SKD11, in which open and solid symbols represent surface and subsurface crack initiation, respectively. In the bare specimens tempered at 500ºC (SKD11-LT), crack initiates at the specimen surface

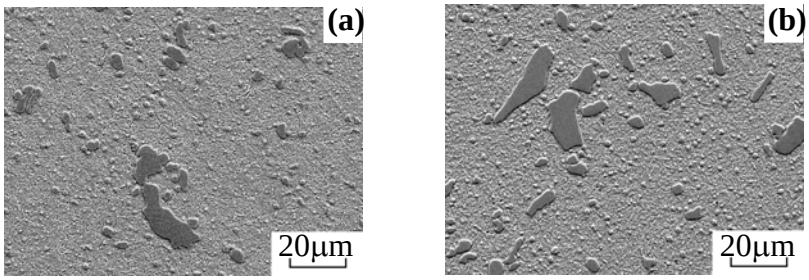

Fig.1 Microstructures of SKD11: (a) LT, (b) HT.

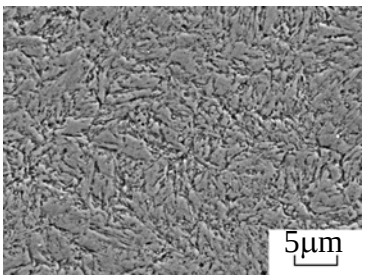

Fig.2 Microstructure of SKD61.

when the stress amplitude, σ, is higher than 1000MPa, while initiates internally when σ is lower than 900MPa. This kind of step-wise *S-N* diagram is typically seen in high strength steels [2]. The fatigue strengths of the specimens with thin DLC film (LT-DLC1) coincide with those of bare ones. However, subsurface crack initiation occurs in LT-DLC1 at the stress amplitudes of 1000MPa and 1100MPa, where surface crack initiation is exclusively dominant in the bare specimens. The fatigue strengths of the specimens with thick DLC film (LT-DLC15) are similar to those with thin DLC film, where crack initiates internally at the stress amplitude of 1000MPa. It indicates that DLC film induced the transition from surface to subsurface crack initiation mechanism at high stress levels and resulted in the higher fatigue strength of DLC coated specimens than bare ones at those stress levels.

In the bare specimens tempered at 600ºC (SKD11-HT), only surface crack initiation is seen regardless of stress levels due to the lower hardness and compressive residual stress than SKD11-LT. The crack initiation mechanism and fatigue strengths of the specimens with thin DLC film (HT-DLC1) are the same as the bare ones. On the contrary, the specimens with thick DLC film (HT-DLC15) show much higher fatigue strengths than the others. In addition, thick DLC film alone induces the transition from surface to subsurface crack initiation mechanism, and consequently fatigue strengths are highly improved. It should be noted that crack initiates on the specimen surface at σ = 800MPa in HT-DLC15, while the fatigue strength is still higher compared with that of the bare one with surface crack initiation.

3.2.2 Fractographic analysis

SEM micrographs showing crack initiation sites of the bare specimens (LT), LT-DLC1 and LT-DLC15 are revealed in Figs.4~6, respectively. In the bare specimens, crack initiates from the large carbide at the surface at high stress level (Fig.4(a)), while typical fish-eye fracture surface is seen at low stress level

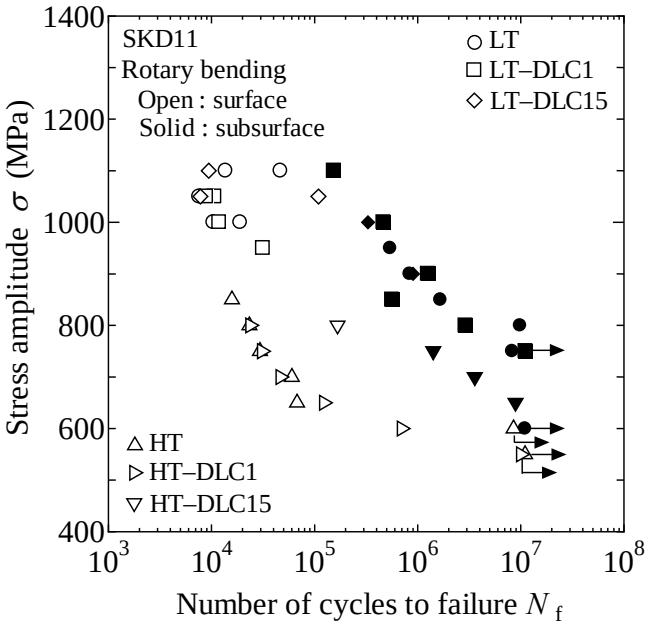

Fig.3 *S-N* diagram of SKD11.

(Fig.4(b)) indicating crack initiated from subsurface carbide. In both LT-DLC1 and LT-DLC15, crack initiation from subsurface carbide is recognized even at the high stress levels of 1100MPa (Fig.5(a)) and 1050MPa (Fig.6(a)), where surface crack initiation was exclusively observed in the bare specimens.

Figs.7(a), (b) reveal the crack initiation sites of the bare (HT) and thin DLC coated (HT-DLC1) specimens, respectively. In both specimens crack initiates from the carbide at the specimen surface irrespective of stress level. On the other hand, crack initiates from the subsurface carbide at low stress level of 650MPa in the thick DLC coated specimen (HT-DLC15) as shown in Fig.8(b). In all fractured specimens, the size of carbide at the crack initiation site was about 35~60μm, and crack initiated due to the brittle fracture of carbide.

3.3 SKD61

3.3.1 Fatigue strength

Fig.9 represents *S*-*N* diagram of SKD61. In the bare specimens, crack dominantly initiates at the specimen surface with an exception at σ = 750MPa where crack initiated internally. In this case, it was found that the inclusion at the subsurface crack initiation site was very close to the specimen surface. The specimens with

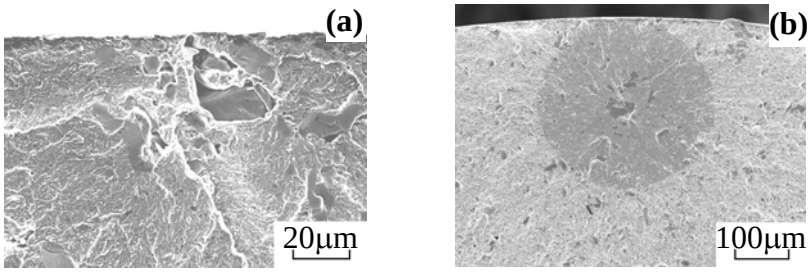

Fig.4 SEM micrographs showing crack initiation site in SKD11-LT:
(a) σ=1000MPa, (b) σ=900MPa.

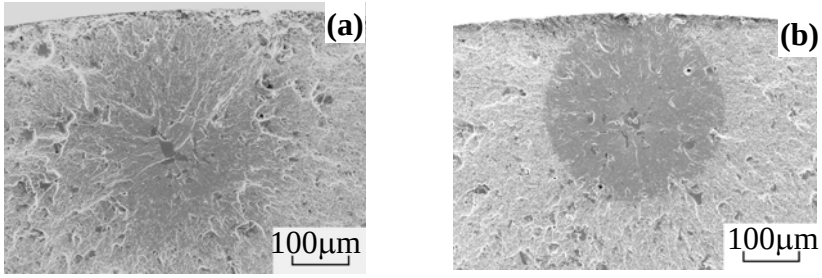

Fig.5 SEM micrographs showing crack initiation site in SKD11-LT-DLC1:
(a) σ=1100MPa, (b) σ=900MPa.

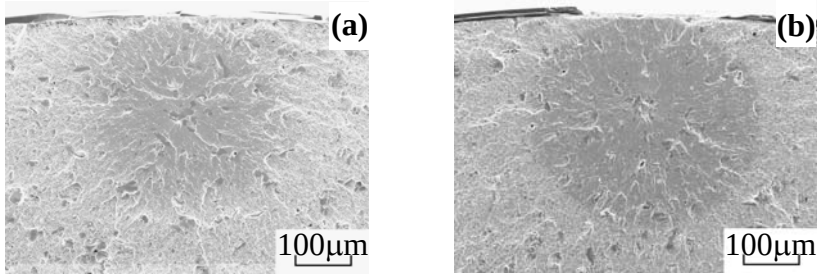

Fig.6 SEM micrographs showing crack initiation site in SKD11-LT-DLC15:
(a) σ=1050MPa, (b) σ=900MPa.

thin DLC film (DLC1) show slightly higher fatigue strengths than bare ones at the stress levels where surface crack initiation is dominant. Subsurface crack initiation is recognized at σ = 750MPa in DLC1. In the specimens with thick DLC film (DLC15), fatigue strengths are further improved and subsurface crack initiation is seen at higher stress levels of σ = 800MPa, 850MPa and 900MPa. It should be noted that fatigue strengths are highly improved by DLC film.

3.3.2 Fractographic analysis

SEM micrographs showing crack initiation sites of bare specimens, DLC1 and

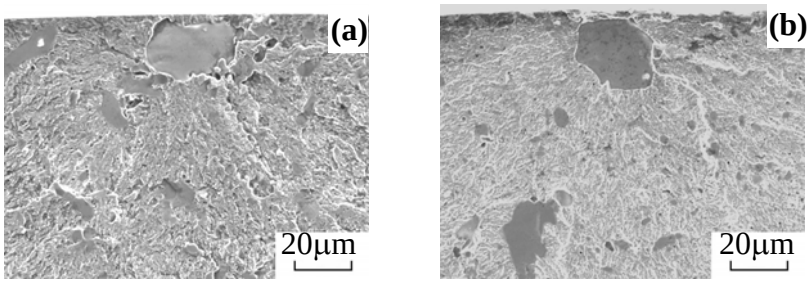

Fig.7 SEM micrographs showing crack initiation site: (a) SKD11-HT (σ=700MPa), (b) SKD11-HT-DLC1 (σ=650MPa)

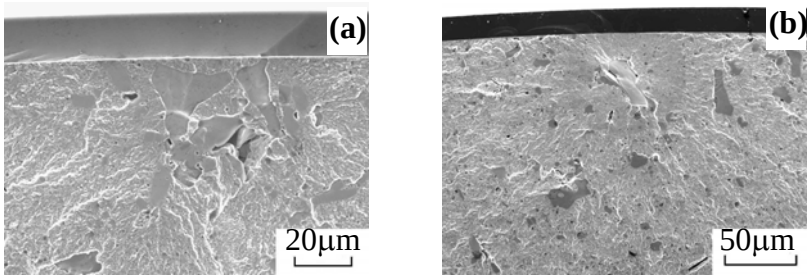

Fig.8 SEM micrographs showing crack initiation site in SKD11-HT-DLC15: (a) σ=800MPa, (b) σ=650MPa

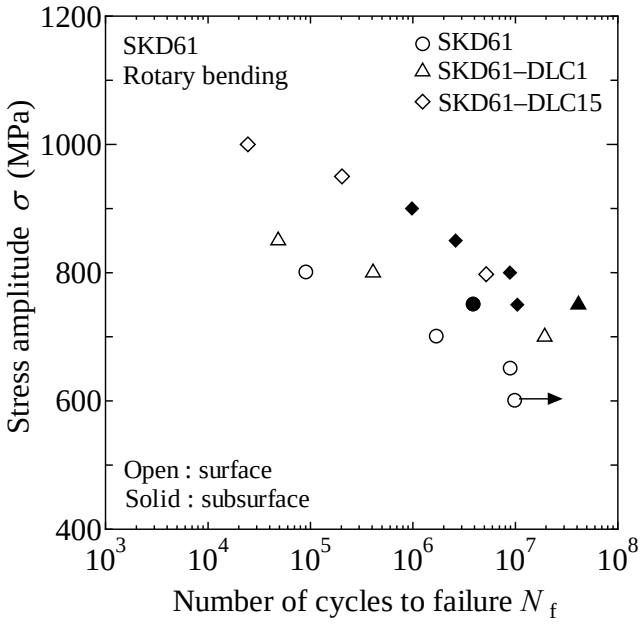

Fig.9 *S-N* diagram of SKD61.

DLC15 are shown in Figs.10~12, respectively. In the bare specimen, crack initiates from the inclusion at the specimen surface at high stress level (Fig.10(a)), while initiates form the subsurface inclusion at low stress level (Fig.10(b)). In Fig.10(b), however, the inclusion is very close to the specimen surface, and consequently fish-eye is not clearly recognized. In DLC1 and DLC15, crack initiates from the inclusion at the specimen surface at high stress levels (Figs.11(a) and 12(a)), while typical fish-eye due to the crack initiation from subsurface inclusion is recognized at low stress levels (Figs.11(b) and 12(b)). The size of inclusion is about 30~45μm and slightly smaller than the carbides recognized at the crack initiation sites in SKD11. The inclusion of SKD61 was identified as calcium oxide by EDX analysis.

4. Discussion

4.1 Fatigue behaviour of bare material

In the bare specimens, crack initiation from surface carbide or inclusion was dominant in SKD11-HT and SKD61, while subsurface crack initiation was exclusively seen at low stress levels in SKD11-LT. It is considered that higher

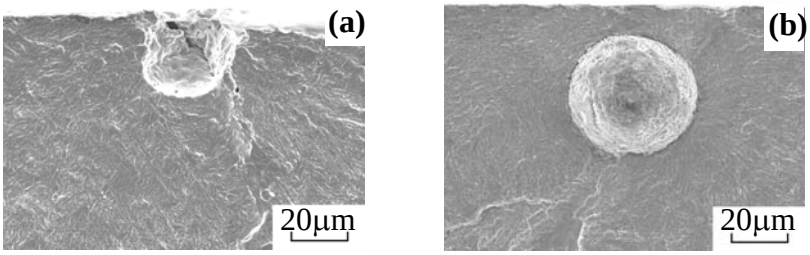

Fig.10 SEM micrographs showing crack initiation site in SKD61:
(a) σ=800MPa, (b) σ=750MPa.

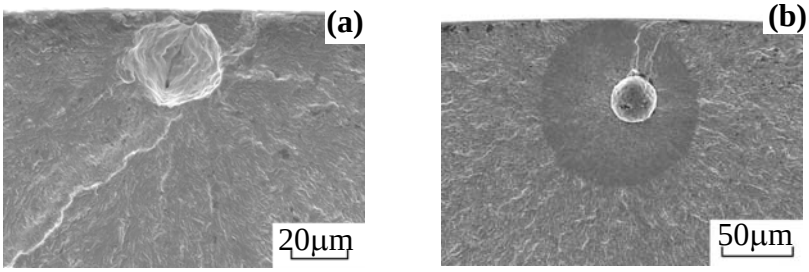

Fig.11 SEM micrographs showing crack initiation site in SKD61-DLC1:
(a) σ=800MPa, (b) σ=750MPa.

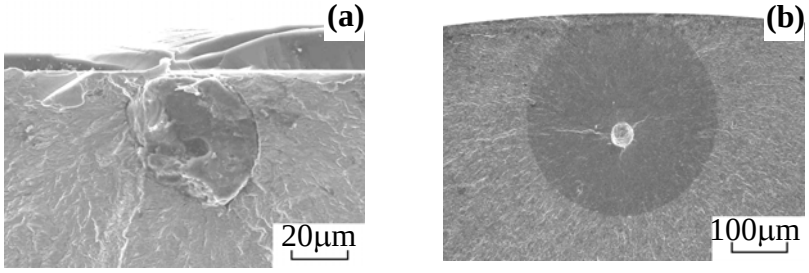

Fig.12 SEM micrographs showing crack initiation site in SKD61-DLC15:
(a) σ=1000MPa, (b) σ=800MPa.

hardness and compressive residual stress of SKD11-LT resulted in the subsurface crack initiation.

4.2 Effect of DLC film on fatigue behaviour

4.2.1 Surface crack initiation

S-N curves resulted from surface crack initiation are shown by open symbols in Figs.3 and 9. In those curves of open symbols, the effect of DLC film was not seen in SKD11-LT, while the fatigue strength was enhanced by 15μm DLC film in SKD11-HT (Fig.3). The effect of DLC film was clearly recognized in SKD61 where the fatigue strength was increased with increasing film thickness (Fig.9). In SKD11, surface crack initiation was due to the brittle fracture of large carbides as shown in Figs.4~8. It is considered that DLC film could not restrict the fracture of carbide, i.e. crack initiation, regardless of film thickness in SKD11-LT, because carbides are fairly large and also applied load level is high. In SKD11-HT, crack initiation was still due to the brittle fracture of large carbides, while applied load levels were lower than SLD11-LT due to the softer matrix. Therefore, only thick DLC film could restrict crack initiation and resulted in the higher fatigue strength.

In SKD61, surface crack initiation was not due to the brittle fracture of inclusion but the slip deformation around inclusion which brought about the fracture at the interface of inclusion. In addition, the size of inclusion was smaller than the carbides in SKD11 and the applied load level was lower than SKD11-LT. Consequently, the clear dependence of fatigue strength on the film thickness was seen, as schematically shown by an arrow, I, in Fig.13, where fatigue strength increased with increasing film thickness.

4.2.2 Subsurface crack initiation

S-N curves resulted from subsurface crack initiation are indicated by solid symbols in Figs.3 and 9. The effect of DLC film on those *S-N* curves is not seen irrelevant to materials. This is because the size of fish-eye was about 300μm as shown in fractographic analyses and DLC film whose thickness of 1 or 15μm

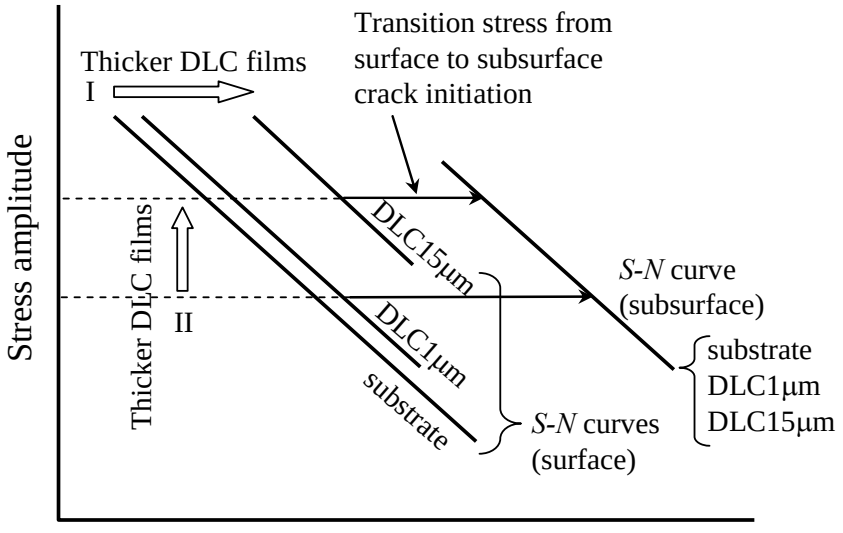

Fig.13 Schematic illustration of the effect of DLC film on fatigue behaviour.

could not restrict crack growth on the specimen surface.

4.2.3 Transition of fatigue crack initiation mechanism

In both materials, SKD11 and SKD61, DLC film induced subsurface crack initiation at high stress levels where surface crack initiation was dominant in bare specimens. It is considered that hard DLC film with good adhesion to the substrate constrained crack initiation at the specimen surface and resulted in the transition from surface to subsurface crack initiation mechanism. Subsurface crack initiation could easily occur in SKD11-LT due to higher hardness and compressive residual stress. Therefore thin DLC film could induce subsurface crack initiation at high stress levels. On the contrary, only thick DLC film could have brought about subsurface crack initiation in SKD11-HT with low hardness. In SKD61, the transition occurred in both specimens with thin and thick DLC films. But the transition stress increased with increasing film thickness as schematically shown by an arrow, II, in Fig.13. It can be concluded that DLC film could improve fatigue strength of die materials due to the transition of crack initiation mechanism and the thicker film was more effective.

5. Conclusions

In this study, DLC films were deposited on SKD11 tempered at 500ºC and 600 ºC and SKD61 tempered at 600ºC with two different film thicknesses of 1μm and 15μm. Rotary bending fatigue tests were conducted in order to investigate the effect of DLC film on fatigue behaviour. The following results are obtained.

1. In SKD11 tempered at 500ºC, surface and subsurface crack initiation occurred at high and low stress levels, respectively. Both thin and thick DLC films induced subsurface crack initiation at high stress levels where surface crack initiation was exclusively seen in the bare specimens, and resulted in the higher fatigue strength of DLC coated specimens. DLC film had no effect on the fatigue strength resulted from subsurface crack initiation.
2. In SKD11 tempered at 600ºC, surface crack initiation was dominant in bare specimens due to lower hardness. Only thick DLC film could induce subsurface crack initiation and resulted in the higher fatigue strength.
3. In SKD61 tempered at 600ºC, surface crack initiation was dominant in bare specimens. The fatigue strengths of DLC coated specimens increased with increasing film thickness. DLC film induced the transition from surface to subsurface crack initiation, and the transition stress increased with increasing film thickness.

References

[1] J.C. Sa´nchez-Lo´pez a, C. Donnet, J. Fontaine, M. Belin, A. Grill, V. Patel, C. Jahnes, Diamond-like carbon prepared by high density plasma, Diamond and Related Materials, 9 (2000) 638–642

[2] H. Itoga, K. Tokaji, M. Nakajima, H.-N. Ko, Effect of surface roughness on step-wise *S–N* characteristics in high strength steel, Int J Fatigue 25 (5) (2003) 379-385